JOURNAL OF SOLID STATE CHEMISTRY 86, 286–292 (1990)

Solid State Studies on Rhodium-Substituted $CuCr_2O_4$ Spinel Oxide

NALINI PADMANABAN, B. N. AVASTHI, AND J. GHOSE[1]

Chemistry Department, Indian Institute of Technology, Kharagpur 721302, India

Received June 5, 1989; in revised form January 22, 1990

Rhodium-substituted $CuCr_2O_4$, i.e., $CuCr_{2-x}Rh_xO_4$, spinel oxides were prepared. X-ray analysis showed that single phase spinels were obtained for $x = 0$ to 0.8, 1.8, and 2.0. The other samples had an additional $Cu_2Cr_2O_4$ phase. The temperature variation of electrical resistivity for all the single phase samples except $CuRh_2O_4$ was similar to that of $CuCr_2O_4$ and with the substitution of Cr (3*d* transition metal) by Rh (4*d* transition metal) the conduction process did not change gradually from $CuCr_2O_4$ type to $CuRh_2O_4$ type. © 1990 Academic Press, Inc.

Introduction

The spinel oxide, $CuRh_2O_4$, is a tetragonally distorted normal spinel at room temperature and, similar to $CuCr_2O_4$, undergoes a tetragonal → cubic phase transition above 800 K (*1*). The cubic phase above 800 K was detected by high-temperature X-ray studies and the magnetic studies showed some anomaly around 800 K. However, the electrical studies did not show any unusual behavior near the phase transition temperature (*2*). This is unlike the observations made on some other spinels in which crystallographic phase transitions have been found to give rise to interesting electrical properties (*3–9*). The spinel oxides $CuCr_2O_4$ (*3*), $Cu_xMn_{3-x}O_4$ (*4*), $Cd_xCu_{1-x}Mn_2O_4$, $Co_xCu_{1-x}Mn_2O_4$ (*5*), $Mg_xCu_{1-x}Cr_2O_4$, and $CuCr_{2-x}Al_xO_4$ (*8*) show the presence of a hysteresis loop in the log ρ vs $1/T$ heating and cooling plots near their phase transition temperatures. But the plots of $CuRh_2O_4$ (*2*) show no such hysteresis loop. Both $CuCr_2O_4$ and $CuRh_2O_4$ are tetragonally distorted due to the presence of Cu^{2+} ions on the tetrahedral site of the spinel lattice and any dissimilarity in the properties of these two oxides could be due to the octahedral site cations, chromium (a 3*d* transition metal cation), and rhodium (a 4*d* transition metal cation). Thus the present work was taken up to study the electrical behavior of $CuCr_2O_4$ samples where chromium is progressively replaced by rhodium.

Experimental

Sample Preparation

The series of $CuCr_{2-x}Rh_xO_4$ ($x = 0$, 0.2, 0.6, 0.8, 1.0, 1.4, 1.6, 1.8, and 2.0) solid solution samples were prepared by adding stoichiometric amounts of Rh_2O_3 (Johnson and Mathey) to a solution containing stoichiometric amounts of cupric nitrate (BDH, Analar Grade) and chromium nitrate (Fluka). The resulting mixture was evapo-

[1] To whom correspondence should be addressed.

0022-4596/90 $3.00

TABLE I

SAMPLE PREPARATION

Sample	Code	Sintering		Annealing	
		Temperature	Time	Temperature	Time
$CuCr_2O_4$	NR 0	1073 K	12 hr	973 K	12 hr
$CuCr_{1.8}Rh_{0.2}O_4$	NR 2	1173 K	24 hr	973 K	24 hr
$CuCr_{1.4}Rh_{0.6}O_4$	NR 6	1173 K	24 hr	973 K	24 hr
$CuCr_{1.2}Rh_{0.8}O_4$	NR 8	1173 K	24 hr	973 K	24 hr
$CuCr_{1.0}Rh_{1.0}O_4$	NR 10	1173 K	24 hr	973 K	30 hr
$CuCr_{0.6}Rh_{1.4}O_4$	NR 14	1174 K	36 hr	973 K	60 hr
$CuCr_{0.4}Rh_{1.6}O_4$	NR 16	1173 K	48 hr	973 K	90 hr
$CuCr_{0.2}Rh_{1.8}O_4$	NR 18	1173 K	48 hr	973 K	24 hr
$CuRh_2O_4$	NR 20	1173 K	48 hr	973 K	24 hr

rated to dryness and decomposed at 973 K to obtain the corresponding oxides. The oxide mixture was then ground thoroughly in an agate mortor and made into pellets under a pressure of 10 tons/cm^2. The pellets were fired in air at 1173 K, slowly cooled to 973 K, and annealed for several hours. Subsequently the samples were cooled to room temperature at the rate of 2 K/min. Details of the heat treatment for individual samples are given in Table I.

X-ray Diffraction Studies

X-ray diffraction analyses of all the samples were carried out using a Philips Model PW1710/00 X-ray diffraction unit. A copper target with Nickel filter was used for all the samples. The lattice parameters (a_0 and c_0) were calculated by the graphical method of indexing powder patterns of tetragonal crystals formulated by Hull and Davey (*10*).

Electrical Resistivity Measurements

The samples were pressed into pellets of 3 mm thickness under a pressure of 10 tons/cm^2 and annealed at 873 K for 6 hr prior to each measurement. The resistivities of these pellets were determined in air between 373 and 923 K using a two-probe technique described elsewhere (*3*).

Thermoelectric Power Measurements

The reduced thermoelectric power at room temperature was measured using a setup described elsewhere (*11*). The temperature T and temperature gradient ΔT were measured using a Chromel–Alumel thermocouple while the ΔV was measured using Pt leads.

Results

X-ray diffraction patterns showed all samples to be tetragonal spinels (Figs. 1 and 2). The lattice parameters and c/a values for the spinel phase of the samples are given in Table II. Table III lists the X-ray lines of the various phases present in the multiphase samples. Figure 3 shows the variations of lattice parameter and the cube root of unit cell volume of the spinel phase with composition.

The log ρ vs $1/T$ heating and cooling plots are shown in Figs. 4–6. All the heating curves (except for NR 18 and NR 20) show linear behavior up to a certain temperature above which nonlinearity sets in and on cooling a hysteresis loop appears. In Figs. 6c and 6d the heating curves for NR 18 and NR 20 show a distinct break in the linear plots and also NR 20 does not show a hys-

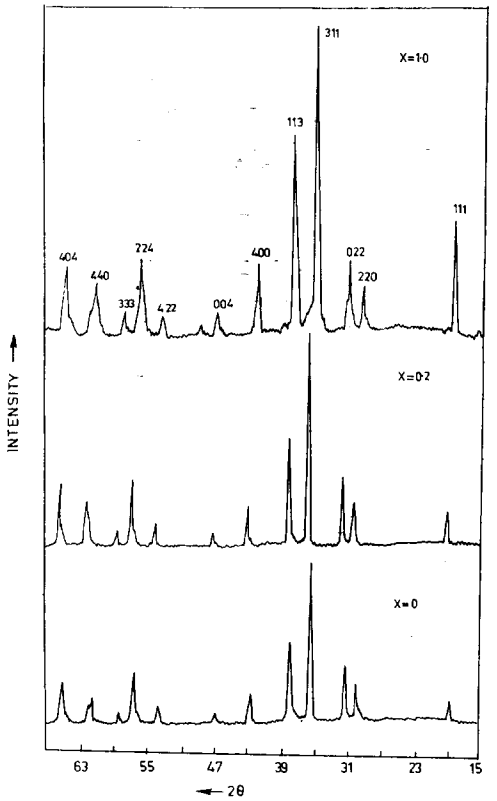

FIG. 1. X-ray diffractograms of $CuCr_{2-x}Rh_xO_4$.

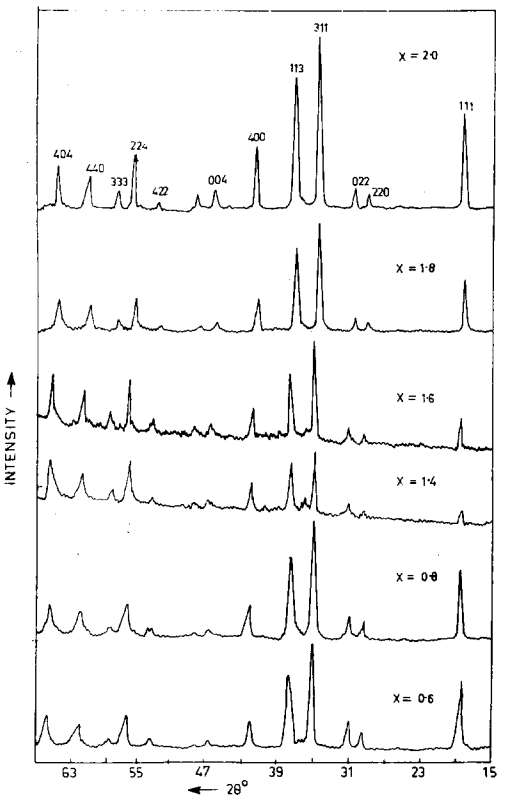

FIG. 2. X-ray diffractograms of $CuCr_{2-x}Rh_xO_4$.

teresis loop on cooling. However, in all the samples the heating and cooling plots are reversible except in the temperature region where the hysteresis loop appears.

The results of the thermoelectric power measurements show that all the samples are *p*-type at room temperature.

Discussion

The X-ray patterns in Figs. 1 and 2 show that all the $CuCr_{2-x}Rh_xO_4$ (x = 0 to 2) solid solution samples form tetragonally distorted spinel oxides. However, samples with x = 1 (NR 10), 1.4 (NR 14), and 1.6 (NR 16) are not single phase as their patterns show some weak extra lines which could be identified with $Cu_2Cr_2O_4$ and Rh_2O_3 lines (Table III). Also, the patterns of NR 14 and NR 16 show that the spinel lines are not very well defined although these samples were sintered and annealed

TABLE II

c_0, a_0, AND c_0/a_0 FOR THE SPINEL PHASE SAMPLES IN THE $CuCr_{2-x}Rh_xO_4$ SYSTEM

Sample	c_0 in Å (±0.003)	a_0 in Å (±0.003)	c_0/a_0
NR 0	7.751	8.489	0.913
NR 2	7.750	8.524	0.909
NR 6	7.763	8.564	0.907
NR 8	7.781	8.576	0.907
NR 10	7.801	8.592	0.907
NR 14	7.822	8.623	0.907
NR 16	7.840	8.641	0.907
NR 18	7.888	8.697	0.907
NR 20	7.896	8.700	8.907

TABLE III

IDENTIFICATION OF THE X-RAY LINES IN THE MULTIPHASE SAMPLES

$CuCr_{1.0}Rh_{1.0}O_4$			$CuCr_{0.6}Rh_{1.4}O_4$			$CuCr_{0.4}Rh_{1.6}O_4$		
2θ	Phase	(*hkl*)	2θ	Phase	(*hkl*)	2θ	Phase	(*hkl*)
18.67	Spinel	(111)	18.6	Spinel	(111)	18.76	Spinel	(111)
29.54	Spinel	(210)	29.52	Spinel	(220)	29.44	Spinel	(220)
31.08	Spinel	(022)	31.06	Spinel	(022)	31.1	Spinel	(022)
31.44	$Cu_2Cr_2O_4$	(006)				31.76	$Cu_2Cr_2O_4$	(006)
35.0	Spinel	(311)	35.0	Spinel	(311)	35.02	Spinel	(311)
36.2	$Cu_2Cr_2O_4$	(012)	36.0	$Cu_2Cr_2O_4$	(012)	36.0	$Cu_2Cr_2O_4$	(012)
37.64	Spinel	(113)	37.62	Spinel	(113)	37.73	Spinel	(113)
			40.8	$Cu_2Cr_2O_4$	(104)	40.6	$Cu_2Cr_2O_4$	(104)
42.12	Spinel	(400)	42.0	Spinel	(400)	42.0	Spinel	(400)
46.72	Spinel	(004)	46.74	Spinel	(004)	46.6	Spinel	(004)
48.6	Spinel[a]	(133)	48.4	Spinel[a]	(133)	48.4	Spinel[a]	(133)
53.04	Spinel	(422)	52.98	Spinel	(422)	53.0	Spinel	(422)
55.76	Spinel	(224)	55.6	Spinel	(224)	55.6	Spinel	(224)
57.64	Spinel	(333)	57.4	Spinel	(333)	57.6	Spinel	(333)
60.96	Spinel	(440)	60.8	Spinel	(440)	60.6	Spinel	(440)
61.48	Spinel[a]	(115)	61.2	Spinel[a]	(115)	61.2	Spinel[a]	(115)
							Rh_2O_3	(314)
64.48	Spinel	(404)	64.4	Spinel	(404)	64.22	Spinel	(404)

[a] Spinel peaks not identified in the X-ray patterns.

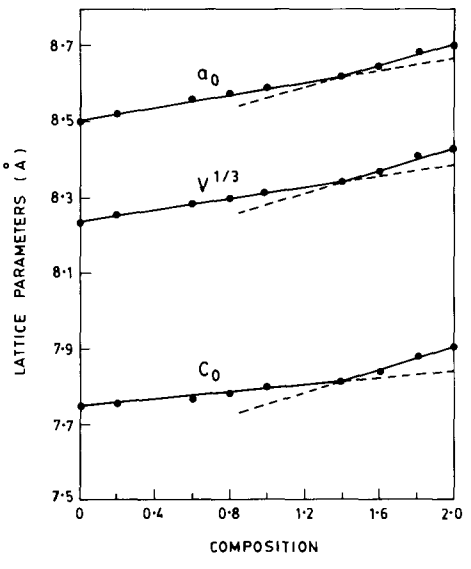

FIG. 3. Variation of lattice parameters, cube root of unit cell volume with composition x for $CuCr_{2-x}Rh_xO_4$.

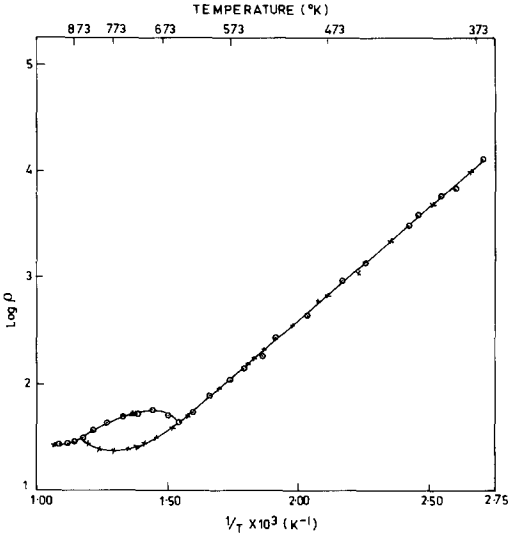

FIG. 4. Heating (o) and cooling (x) plot of log specific resistivity versus absolute temperature for $CuCr_2O_4$.

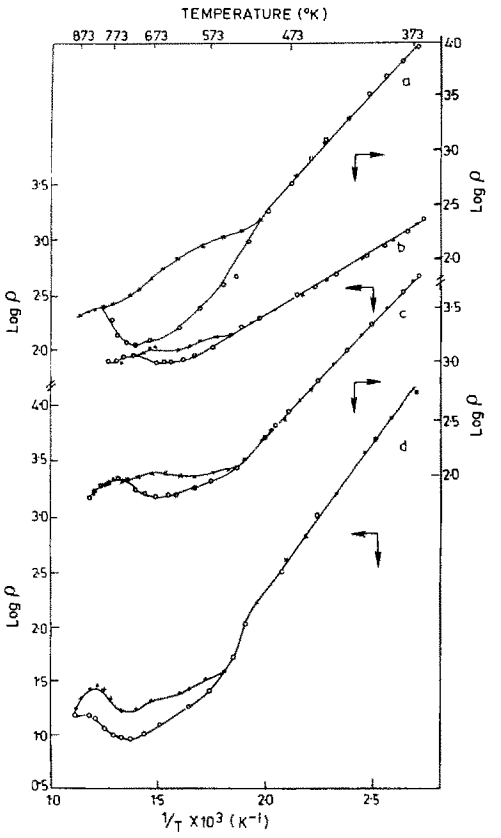

FIG. 5. Heating (o) and cooling (x) plots of log specific resistivity versus absolute temperature for (a) $CuCr_{0.6}Rh_{1.4}O_4$, (b) $CuCr_{0.4}Rh_{1.6}O_4$, (c) $CuCr_{0.2}Rh_{1.8}O_4$, (d) $CuRh_2O_4$.

for longer periods (Table I). These results indicate that with increasing amounts of rhodium substitution in $CuCr_2O_4$, the formation of single phase spinel becomes more difficult. But the ease with which single phase spinel samples were formed for $x = 1.8$ and 2.0 shows that small amounts of chromium can be introduced into the $CuRh_2O_4$ spinel lattice without much difficulty. Thus, a complete solid solution of $CuCr_2O_4$ and $CuRh_2O_4$ is not possible and hence a break is observed in the lattice parameter vs composition linear plot (Fig. 3). Difficulty in obtaining a complete solid solution has also been reported for $CuFe_2O_4$–$CuRh_2O_4$ (*12*) and $CuRh_2O_4$–$NiRh_2O_4$ (*13*) systems which suggests that copper rhodium spinel oxides probably have difficulty in forming a complete solid solution with other spinel oxides.

Figures 5 and 6 show that for most of the samples the log ρ vs $1/T$ heating curve is linear and is retraced by the cooling curve up to a certain temperature. The nonlinear curve at higher temperatures form a hysteresis loop with the cooling curve. This is similar to the log ρ vs $1/T$ plots of $CuCr_2O_4$ (Fig. 4) in which the hysteresis loop was attributed to a first order, reversible diffusionless, tetragonal → cubic phase transition. In the aluminium- and magnesium-substituted $CuCr_2O_4$ samples, hysteresis

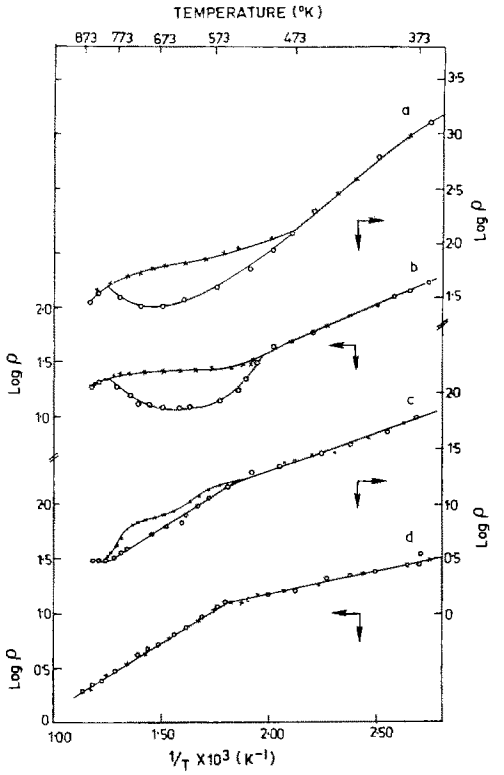

FIG. 6. Heating (o) and cooling (x) plots of log specific resistivity versus absolute temperature for (a) $CuCr_{1.8}Rh_{0.2}O_4$, (b) $CuCr_{1.4}Rh_{0.6}O_4$, (c) $CuCr_{1.2}Rh_{0.8}O_4$, (d) $CuCr_{1.0}Rh_{1.0}O_4$.

loops in the log ρ vs $1/T$ heating and cooling plots were observed in tetragonal samples undergoing cubic phase transition and were absent in cubic samples not undergoing any phase transition (*8*). In the present studies, the presence of hysteresis loops in all the samples (except $CuRh_2O_4$) may imply that rhodium-substituted $CuCr_2O_4$ spinels which are tetragonal at room temperature probably undergo a cubic phase transition on heating, similar to the aluminium- and magnesium-substituted tetragonal $CuCr_2O_4$ samples (*8*).

High temperature X-ray studies on $CuRh_2O_4$ have shown that it undergoes a tetragonal to cubic phase transition between 800 and 850 K (*1*), but as reported by Murthy and Ghose (*2*) and also shown in the present studies, this phase transition of $CuRh_2O_4$ is not accompanied with any hysteresis loop in the log ρ vs $1/T$ heating and cooling plots. Murthy and Ghose attributed this behavior of $CuRh_2O_4$ to the presence of rhodium which is a 4*d* transition metal element. This is justified as all the other spinels showing a hysteresis loop near the phase transition temperature have only 3*d* transition metal ions in the spinel lattice (*3, 5, 8, 9*).

Conduction in the spinel oxides is thought to be by hopping of charge carriers (*14*) and is sensitive to any change in the distance between the cations involved in the hopping process (*15, 16*). Thus during tetragonal to cubic phase transition in a spinel oxide, where the lattice parameters change, there is a possibility of a change in the distance between the cations which should be reflected in their conduction process. But if conduction is by a mechanism which is insensitive to any change in cation–cation distance then phase transition cannot be studied by conductivity measurements. Thus, the absence of a hysteresis loop in the log ρ vs $1/T$ plot of $CuRh_2O_4$, near its phase transition temperature, may indicate that unlike most of the 3*d* transition metal spinel oxides, conduction in $CuRh_2O_4$ is probably not by hopping of charge carriers.

The ln ρ vs $1/T$ plot of NR 18 (Fig. 6c) presents some interesting results. Although it shows a hysteresis loop, the heating plot does not become nonlinear in the hysteresis loop region as found with the other rhodium-substituted $CuCr_2O_4$ samples. The plot is linear in the studied temperature region with a break at higher temperatures similar to the $CuRh_2O_4$ plot (Fig. 6d). But after phase transition, during cooling, the plot is nonlinear in the hysteresis loop region. The presence of a hysteresis loop in the log ρ vs $1/T$ heating and cooling plots is similar to the observations of other 3*d* transition metal spinel oxides undergoing tetragonal to cubic phase change and hence it appears that, although this spinel contains a small proportion of 3*d* transition metal cation, its conduction process is not altogether similar to $CuRh_2O_4$. Thus in a spinel-like $CuCr_{2-x}Rh_xO_4$ where both 3*d* and 4*d* transition metal ions are present, the contribution of the octahedral site 3*d* transition metal cation toward the conduction process seems to be dominant and hence the log ρ vs $1/T$ plot of $CuCr_{1.8}Rh_{0.2}O_4$ (Fig. 5a) is similar to $CuCr_2O_4$ (Fig. 4) but the plot of $CuCr_{0.2}Rh_{1.8}O_4$ (Fig. 6c) is only partially similar to $CuRh_2O_4$ (Fig. 6d). From these results it may be concluded that in a spinel like $CuCr_{2-x}Rh_xO_4$, where the 3*d* transition metal cation Cr^{3+} is progressively replaced by a 4*d* transition metal ion, Rh^{3+}, the conduction process does not change gradually from $CuCr_2O_4$ type to $CuRh_2O_4$ type and the 3*d* transition metal cation in the spinel lattice dominates the conduction process.

Acknowledgment

The authors thank DST for some financial assistance.

References

1. G. BLASSE, *Philips Res. Rept.* **18,** 383 (1963).
2. K. S. R. C. MURTHY AND J. GHOSE, *J. Solid State Chem.* **71,** 441 (1987).
3. K. S. DE, J. GHOSE, AND K. S. R. C. MURTHY, *J. Solid State Chem.* **43,** 261 (1982).
4. M. ROSENBERG, P. NICOLAU, AND I. BUNGET, *Phys. Status Solidi* **15,** 521 (1966).
5. S. T. KHIRSAGAR AND C. D. SABANE, *Japan J. Appl. Phys.* **10,** 794 (1971).
6. M. ROSENBERG, *J. Phys. Chem. Solids* **24,** 1419 (1963).
7. R. METSELAAR, R. E. T. VANTOL, AND A. PIERCY, *J. Solid State Chem.* **38,** 335 (1981).
8. K. S. DE, J. GHOSE, AND K. S. R. C. MURTHY, *J. Solid State Chem.* **47,** 264 (1983).
9. M. ROSENBERG, P. NICOLAU, R. MANAILA, AND P. PAUSESCU, *J. Phys. Chem. Solids* **24,** 1419 (1963).
10. B. D. CULLITY, "Elements of X-Ray Diffraction," p. 331, Addison–Wesley, Reading, MA (1978).
11. N. PADMANABAN, B. N. AVASTHI, AND J. GHOSE, *J. Solid State Chem.* **81,** 250 (1989).
12. G. BLASSE, *Philips Res. Rept. Suppl.* **64,** 3 (1964).
13. J. DULAC, *Bull. Soc. Fr. Mineral. Cristallogr.* **92,** 25 (1969).
14. J. P. SUCHET, "Electrical Conduction in Solid Materials," p. 55, Pergamon, New York (1975).
15. P. POMONIS AND J. C. VICKERMAN, *J. Catal.* **55,** 88 (1978).
16. D. ADLER, "Solid State Physics," Vol. 21, p. 1, Academic Press, New York (1968).